Journal of Diabetes and Its Complications 33 (2019) 23–32

Contents lists available at ScienceDirect

Journal of Diabetes and Its Complications

journal homepage: WWW.JDCJOURNAL.COM

Endothelial cell-specific overexpression of endothelial nitric oxide synthase in Ins2Akita mice exacerbates diabetic nephropathy☆

Mohan Natarajan [a], Samy L. Habib [b], Robert L. Reddick [a], Caroline R. Delma [a], Krishnan Manickam [a], Thomas J. Prihoda [a], Sherry L. Werner [a], Sumathy Mohan [a,*]

[a] Department of Pathology and Laboratory Medicine, University of Texas Health Science Center at San Antonio, San Antonio, TX, USA
[b] Geriatric Research Education and Clinical Center, South Texas Veterans Healthcare System and Cell Systems & Anatomy, University of Texas Health Science Center at San Antonio, San Antonio, TX, USA

ARTICLE INFO

Article history:
Received 5 April 2018
Received in revised form 13 August 2018
Accepted 7 October 2018
Available online 13 October 2018

Keywords:
Diabetic nephropathy
Endothelial nitric oxide synthase
Nitric oxide
Ins2 Akita type 1 diabetic mice
Reactive oxygen species
Transgenic mice

ABSTRACT

Previous studies demonstrated that global deficiency of eNOS in diabetic mice exacerbated renal lesions and that overexpression of eNOS may protect against tissue injury. Our study revealed for the first time overexpression of eNOS leads to disease progression rather than protection. Transgenic mice selectively expressing eNOS in endothelial cells (eNOSTg) were cross bred with Ins2Akita type-1 (AK) diabetic mice to generate eNOS overexpressing eNOSTg/AK mice. Wild type, eNOSTg, AK and eNOSTg/AK mice were assessed for kidney function and blood glucose levels. Remarkably, overexpressing eNOSTg mice showed evidence of unpredicted glomerular injury with segmental mesangiolysis and occasional microaneurysms. Notably, in eNOSTg/AK mice overexpression of eNOS led to increased glomerular/endothelial injury that was associated with increased superoxide levels and renal dysfunction. Results indicate for the first time that overexpressing eNOS in endothelial cells cannot ameliorate diabetic lesions, but paradoxically leads to progression of nephropathy likely due to eNOS uncoupling and superoxide upsurge. This novel finding has a significant impact on current therapeutic strategies to improve endothelial function and prevent progression of diabetic renal disease. Further, the eNOSTg/AK model developed in this study has significant translational potentials for elucidating the underlying mechanism implicated in the deflected function of eNOS in diabetic nephropathy.

1. Introduction

Diabetes mellitus is a leading cause of chronic kidney disease and end-stage renal disease worldwide.[1] Decreased nitric oxide (NO) bioavailability precedes the development of several complications of diabetes including accelerated atherosclerosis affecting large muscular arteries and diabetic nephropathy resulting from microvascular dysfunction.[2–4] Nitric oxide is generated from the conversion of L-arginine to L-citrulline by isoforms of NOS using tetrahydrobiopterin (BH4) as a cofactor. Among the three isoforms, endothelial (e) NOS is the predominant isoform expressed by vascular endothelial cells that constitutively generates NO. Basal release of eNOS derived-NO maintains endothelial homeostasis that is important for normal vasodilatory tone and thromboresistance.[5–7] In the kidney, NO acts as a potent modulator of renal function and controls vascular tone, glomerular ultrafiltration coefficient and medullary blood flow.[8–10] Under hyperglycemic conditions, excessive reactive oxygen species (ROS) production leads to oxidation of BH4 and eNOS uncoupling, which further enhances cytosolic superoxide generation and reduced NO bioavailability.[11] However, the precise contribution of eNOS/NO activity in promoting kidney lesions in diabetes has not been well-defined.[12]

In previous studies, we generated double-knockout (DKO) mice that have global deletion of the eNOS isoform in a type 2 diabetic *db/db* background.[4] These mice showed increased glomerular injury compared to diabetic and eNOS−/− controls that resembled human diabetic nephropathy. In parallel studies, using mouse models of both type 1 and type 2 diabetes, eNOS deficiency was reported to accelerate nephropathy.[13–16] Based on these findings, we hypothesized that increasing eNOS expression in endothelial cells may be an effective strategy to restore NO bioavailability and prevent progression of diabetic nephropathy.[17] This is supported by work showing that transient overexpression of eNOS by eNOS gene delivery in rats with reduced renal mass improved NO release and prevented a decline in renal function.[18] In addition, overexpression of eNOS in transgenic mice protects against endotoxin shock, neointimal lesion

☆ Disclosure statement: The authors declare that there is no conflict of interest associated with this manuscript.

* Corresponding author at: Department of Pathology and Laboratory Medicine, University of Texas Health Science Center at San Antonio, 7703 Floyd Curl Drive, San Antonio, TX 78229, USA.
E-mail address: mohan@uthscsa.edu (S. Mohan).

https://doi.org/10.1016/j.jdiacomp.2018.10.003
1056-8727/

formation and skeletal muscle ischemic/reperfusion injury.[19–21] In mice with cardiac myocyte-specific overexpression of eNOS, myocardial ischemic/reperfusion injury was also reduced and cardioprotective.[22]

The aim of the present study was to determine if overexpression of eNOS in endothelial cells of type 1 diabetic mice ameliorates diabetic nephropathy. Transgenic mice overexpressing human eNOS protein (eNOSTg) selectively in vascular endothelial cells were cross bred with C57BL6-Ins2^{Akita} type 1 diabetic mice (AK) to generate AK mice with high levels of eNOS (eNOSTg/AK mice). Transgenic eNOS overexpression unexpectedly led to increased glomerular injury and exacerbated diabetic nephropathy in eNOSTg/AK mice resulting in impaired renal function. Increased superoxide levels were detected in eNOSTg and eNOSTg/AK kidneys and likely contributed to increased glomerular injury. These findings provide the first evidence that targeted overexpression of eNOS in endothelial cells potentiates rather than suppresses superoxide production that, in turn, exacerbates diabetic nephropathy. Importantly, the results suggest that optimizing eNOS expression in endothelial cells, perhaps by supplying the substrate L-arginine and/or the cofactor BH4, may be an effective therapeutic modality for preventing glomerular injury and improving renal function in patients with diabetes.

2. Methods

2.1. Animal breeding and genotyping

Type I diabetic C57BL6-Ins2^{Akita}/J (stock number 003548) mice (referred to as AK in this manuscript) were purchased from Jackson Laboratory (Bar Harbor, ME). These mice have an autosomal dominant point mutation in the murine *Ins2* gene that leads to insulin deficiency at birth and elevated blood glucose levels beginning 3 weeks postnatal.[23] AK mice were chosen rather than type 2 *db*/*db* diabetic mice as they are non-obese, fertile mice which facilitates breeding and analysis with age. They are preferred to the streptozotocin (STZ)-induced type I diabetic model which is associated with confounding inflammatory effects.[15,24] Hemizygous AK mice were used for all experiments. Tail snips at the time of weaning were used to identify genotypes using a PCR/restriction length polymorphism assay as previously reported.[25] Transgenic C57BL6 mice expressing human eNOS protein selectively in vascular endothelial cells including glomerular endothelial cells were provided by Dr. Rini de Crom (The Netherlands).[26] To generate AK mice that express human eNOS, hemizygous AK mice were cross bred with hemizygous eNOSTg mice for several generations to ensure genetic homogeneity. Offspring that were positive for both genotypes (hemizygous) are referred to as eNOSTg/AK mice in this manuscript. Mice of both genders averaging from 32 to 40 weeks of age were euthanized and weighed. Physiological parameters were assessed and kidneys from a subset of mice from each group were analyzed for histology. Right and left kidneys were excised and weighed. Blood glucose measurements were performed at the same time of day after 3 h of starvation using the One Touch Ultra Test Strips which have a detection limit of 600 mg/dl. Twenty-four hour urine samples were collected from individually caged mice using Nalgene^{R} metabolic cages (Nalgene Nunc International, Rochester, NY, USA). Urine albumin was measured by mouse albumin ELISA kit from Alpco and creatinine concentrations were measured using QuantiChrom™ Creatinine Assay Kit from BioAssay Systems. IgA levels were determined using a mouse IgA ELISA kit purchased from Thermoscientific (Frederick, MD). Control groups included wild type (WT) C57BL6, eNOSTg (hemizygous) and AK (hemizygous) littermates. All procedures were performed in accordance with National Institutes of Health guidelines with approved protocol by the UTHSCSA Institutional Animal Care and use Committee.

2.2. Immunostaining and Western blot analysis of Total eNOS protein and peroxynitrite in kidneys

Frozen kidneys were homogenized using Tissue protein extraction buffer from Invitrogen (1× HEPES based buffer, pH 7.5). Clear supernatants were obtained after centrifugation of the tissue homogenates at 100,000 xg at 4 °C using Optima Max-TL-ultracentrifuge (Beckman Coulter). Kidney extracts were separated by electrophoresis on a 10% SDS-polyacrylamide gel and then transferred to polyvinyldifluoride membrane (Bio-rad, Hercules, CA) for immunoblot analysis as previously described.[25] Blots were probed with rabbit anti-eNOS antibody or mouse anti-nitrotyrosine monoclonal antibody (Invitrogen). Non-specific protein (NS) or α-tubulin were used as an internal loading control. Fixed kidney sections of 6 μm thickness were also stained with rabbit anti-eNOS antibody (Cell Signaling) and images were captured to show stained endothelial cells of glomerulus and arterioles.

2.3. Determination of eNOS dimerization in kidneys

As eNOS uncoupling is associated with disruption of eNOS dimers and increased monomerization of the enzyme, the dimerization of eNOS in kidney tissue was examined. Frozen kidneys were homogenized with tissue extraction buffer (Invitrogen) containing 1 mM phenylmethylsulfonylfluoride (PMSF), 1× protease inhibitor cocktail at 4 °C and centrifuged at 100,000 rpm for 1 h at 4 °C in a Beckman Coulter Optima Max-TL ultracentrifuge (Beckman Coulter). The supernatants were collected and the protein content was estimated using BCA reagent. Detection of eNOS dimer/monomer levels was performed using low temperature SDS-PAGE (LT-PAGE) and western blotting as previously described.[27]

2.4. Renal histology

Tissue from each kidney was divided and processed as we previously described.[4] Briefly, a section was placed in 10% formalin for paraffin embedding, a separate section was snap frozen in liquid nitrogen for immunofluorescence studies and a small fragment was fixed in 4% formaldehyde/1% glutaraldehyde for electron microscopy. Four μm-thick sections were cut from the paraffin block and stained with hematoxylin & eosin (H&E), periodic acid-Schiff (PAS), methanamine silver or trichrome. Immunofluorescence was evaluated by incubating frozen sections for 1 h with FITC-conjugated rabbit anti-human IgG, IgA, IgM, complement 3 (C3) and complement 1q (C1q) antibodies (1:10 dilution) which cross-react with the corresponding mouse proteins (DakoCytomation, Glostrup, Denmark), followed by washing and mounting. Electron microscopic images and glomerular basement membrane (GBM) measurements were made using the Advanced Microscopy Techniques image capture engine software on a Joel 1230 electron microscope (Peabody, MA). At least 15 different segments of GBM per mouse from three mice were measured in each group and the average GBM thickness (μm) ± SEM was calculated.

2.5. Quantification of renal morphology

Histomorphometric measurements of glomerular volume, cellularity and matrix fraction, and interstitial fibrosis were determined using a computerized image analysis system and Bioquant software (Bioquant Image Analysis Corporation, Nashville, TN) as we previously reported.[4] All quantifications were performed in a blinded manner following the guidelines of animal models of diabetic complications consortium (AMDCC). The average glomerular volume, cellularity and matrix fraction were calculated for each group of mice and expressed as mean ± SEM. Immunofluorescent staining was evaluated in 25–30 glomeruli per mouse and the intensity was evaluated. In coronal sections of the kidney, 200 glomeruli were examined for glomerular injury defined as

any of the following: nodular lesions, mesangiolysis, microaneruysms, perihilar hyaline and segmental sclerosis. The percentage of glomerular injury (Injury index %) was calculated as the number of injured glomeruli divided by total glomeruli. Interstitial fibrosis was calculated as the percent of trichrome blue-positive staining/total tubulointerstitial area (Fibrosis %).

2.6. Superoxide measurements

Fresh kidney samples from WT, eNOSTg, AK and eNOSTg/AK mice were placed in optimal cutting temperature compound (Tissue-Tek ® O.C.T™ Compound Sakura, Torrance, CA) and frozen at −80 °C. 8 μm-thick sections were incubated with dihydroethidium (DHE, 5 μM) for 30 min at 37 °C. Some sections were pre-treated with L-NAME (1 mM), a NOS inhibitor, prior to incubation with DHE for 10 min at 37 °C. DHE staining was visualized using an Olympus IX81 confocal fluorescence microscope. Fluorescent images were captured by Flowview1000 software and quantification was performed using FIJI/ImageJ2 analysis software. DHE signals from each sample (8–10 glomeruli per section from 3 animals/genotype) were calculated.

2.7. Statistical methods

We used analysis of variance (ANOVA) to compare means of the 4 groups (WT, eNOSTg, AK and eNOSTg/AK). This was followed by Fisher's Least Significant Difference multiple comparisons *t*-test for pairwise comparisons. When the residuals were not near normally distributed or variances were unequal, the standard log transform or square root transform was used to obtain improved ANOVA results with assumptions better satisfied. We include reporting of one tailed and two tailed $p < 0.05$ when appropriate.

3. Results

3.1. eNOSTg/AK mice are diabetic

As shown in Table 1, eNOSTg/AK mice were diabetic, and showed elevated blood glucose levels that were not significantly different from AK mice. The ratio of kidney to body weight in eNOSTg was similar to WT, whereas the ratio was increased in AK and eNOSTg/AK mice. Albumin/creatinine (μg/mg) ratio in urine samples of eNOSTg/AK (34 ± 8.27) and AK (73.09 ± 28.02) mice were significantly increased compared to WT (19.9 ± 2.4) mice ($p < 0.05$). Even though the mean value in the eNOSTg group (53.19 ± 29.38) was higher than eNOSTg/AK, it did not gain statistical significance compared to WT. As previously reported[28] none of these genotypes of mice exhibited elevated blood pressure when measured at 24 weeks of age.

3.2. Total eNOS expression in kidneys of eNOSTg and eNOSTg/AK mice

To confirm increased eNOS expression in kidneys of transgenic mice, western blot was performed. As shown in Fig. 1A & B, total eNOS expression was increased in kidneys isolated from eNOSTg mice as well as in kidneys from eNOSTg/AK mice ($^{*}p < 0.05$ compared to WT). In AK mice, basal eNOS expression was reduced in the kidneys compared to WT ($^{**}p < 0.01$) similar to that previously reported in the aorta of AK mice.[25] Immunostained sections of kidneys (Fig. 1C) from eNOSTg and eNOSTg/AK mice show increased eNOS expression in endothelial cells in glomerular capillaries and arterioles compared to WT kidneys. In WT kidneys, an occasional glomerulus shows segmental endothelial staining and weak staining of endothelial cells in arterioles; significant eNOS expression could not be detected in glomeruli and arterioles of AK kidneys. Following low-temperature SDS gel-western blotting, we found high levels of eNOS dimers in wild type kidney extracts (Fig. 1D). Kidney extracts from AK, eNOSTg, and eNOSTg/AK mice showed little or no dimer formation, a feature consistent with uncoupling of eNOS in these mice.

3.3. eNOSTg mice and eNOSTg/AK mice show a spectrum of renal pathology

3.3.1. Glomerular morphology

Compared to WT mice, glomeruli in AK mice showed morphology associated with diabetes including increased volume and matrix expansion (Table 2, Fig. 2a, b).[29] eNOSTg kidney morphology has not been previously reported. Glomeruli in these mice showed increased volume and matrix expansion. Glomerular injury was greater in eNOSTg mice compared to WT or AK mice, and characterized by segmental mesangiolysis (Fig. 2c, arrows) and occasional glomeruli showing microaneurysms, hyaline in the perihilar region and rare sclerotic segments. Mesangiolysis with loss of matrix and microaneurysms are identified on methanamine silver stains (Fig. 2d). In eNOSTg/AK mice, glomeruli showed features that overlapped with eNOSTg and AK glomeruli (increased volume and matrix); however, there was a significant increase in glomerular injury (Table 2) mainly due to increased mesangiolysis and segmental sclerotic lesions which likely correspond to healed lytic segments. eNOSTg/AK glomeruli showed segmental to global mesangiolysis and glomeruli with perihilar hyaline, early nodule formation and sclerotic segments (Fig. 2e-l, silver and PAS stains, arrows); the number of glomeruli with microaneruysms was similar to that in eNOSTg mice. The cellularity of uninjured glomeruli in eNOSTg and eNOSTg/AK mice was similar to WT mice, whereas cellularity was modestly increased in AK mice. In all groups of mice, there was no significant interstitial fibrosis or tubular atrophy, although eNOSTg/AK kidneys showed a trend toward increased fibrosis ($p < 0.08$) (Table 2). In AK and eNOSTg/AK mice, tubules were dilated and contained glycogenated nuclei which have been previously described in diabetic AK mice.

Table 1
Physiological analysis.

Genotype	WT	AK	eNOSTg	eNOSTg/AK
Average age (weeks)	3\2.4 (4.9)	37.0 (5.5)	40.2 (3.6)	33.5 (4.3)
Average blood glucose (mg/dl)[a]	174.8 (12.4)	525.8 (54.7)***	193.0 (16.1)	563.0 (23.4)***
Average body weight (g)	22.1 (0.9)	25.5 (2.5)	27.4 (2.3)	23.7 (1.3)
Average kidney weight (g)[a]	0.15 (0.01)	0.23 (0.03)*	0.19 (0.02)	0.21 (0.01)*
Average of Kidney/body weight $\times 10^{-3}$[a]	6.8 (0.11)	9.3 (1.3)*	7.1 (0.6)	9.0 (0.38)*
Albumin/Creatinine Ratio (μg/mg) in Urine	19.90 (2.40)	73.09 (28.02)*	53.19 (29.38)[b]	34.00 (8.27)*

Data are mean (SEM) for eNOSTg, AK and eNOSTg/AK crossed mice ($n = 5$–7/group). Values are compared with WT (n = 5) and each other using ANOVA followed by Fisher's Least Significant Difference multiple comparisons *t*-tests.

* $p < 0.05$.

*** $p < 0.001$ compared to WT.

[a] eNOSTg vs WT and eNOSTg/Akita vs Akita are not statistically different.

[b] Although higher than eNOSTg/AK, the increased range of values prevented this increase over WT from being significant.

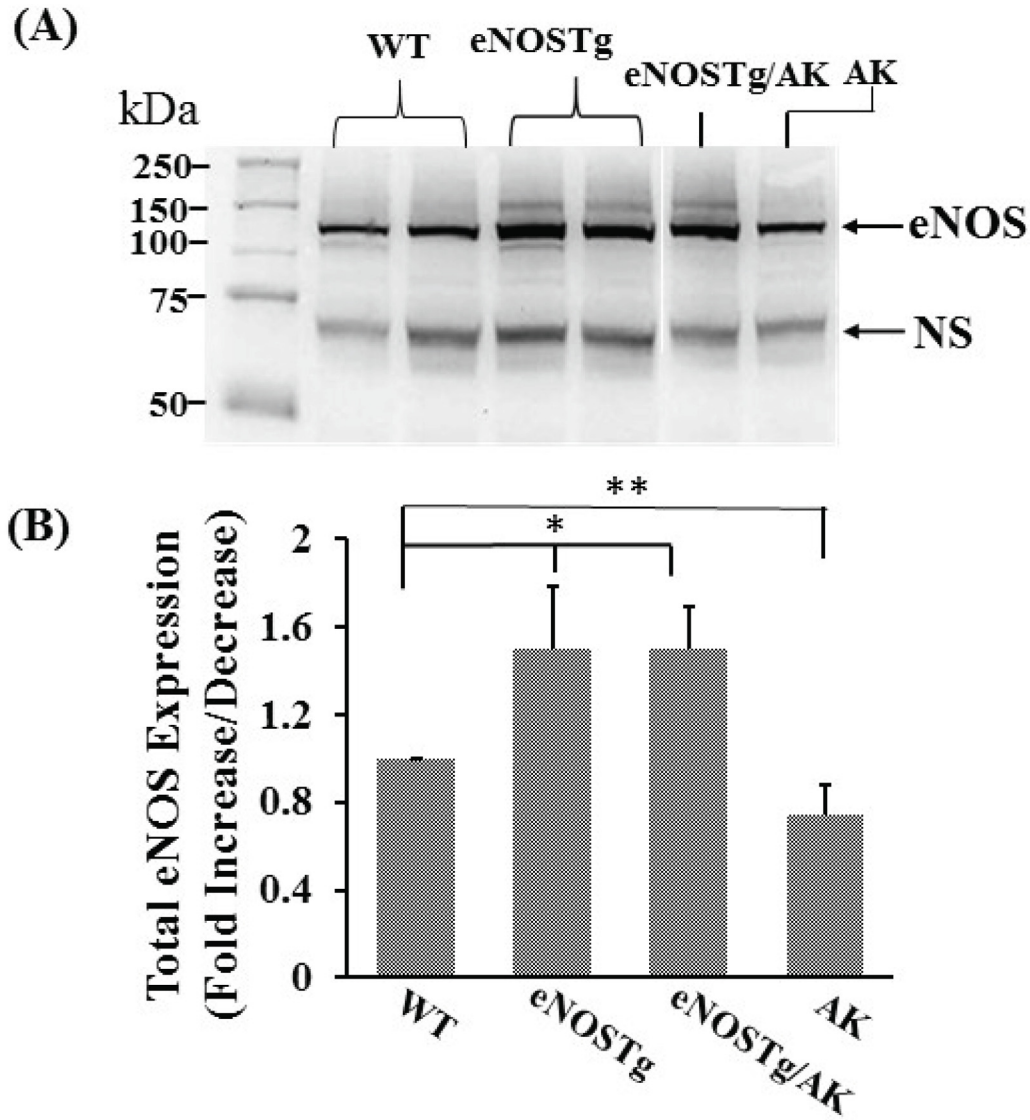
(A)
WT
eNOSTg
eNOSTg/AK
AK
kDa
250
150
100
75
50
eNOS
NS
(B)
Total eNOS Expression
(Fold Increase/Decrease)
2
1.6
1.2
0.8
0.4
0
*
**
WT
eNOSTg
eNOSTg/AK
AK
(C)
WT
eNOSTg
AK
eNOSTg/
AK
Glomeruli
Arterioles

3.3.2. Glomerular ultrastructure

Electron microscopic findings correlated with histology. AK and eNOSTg glomeruli showed increased matrix expansion compared with WT (Fig. 3a-f, arrows). Morphometric analysis also showed a significant increase in GBM thickness in these mice (Table 2). eNOSTg, but not WT or AK, glomeruli showed segments with mesangiolysis characterized by accumulation of electron-lucent material in the mesangium and dissolution of the mesangial matrix (Fig. 3e, f). In some segments, this was associated with endothelial injury with denudation of endothelial cells from the basement membrane. Mesangiolysis and endothelial injury were increased in eNOSTg/AK glomeruli with some segments containing karyorrhexis, platelets and fibrin tactoids. Similar to AK and eNOSTg mice, glomeruli in eNOSTg/AK mice showed increased matrix expansion and thickened GBM (Table 2). In both eNOSTg and eNOSTg/AK glomeruli, some segments showed microaneurysm (MA) formation due to detachment of the GBM from the mesangium (Fig. 3g, asterisks). Osmophilic electron dense deposits were not identified in WT glomeruli. As expected, AK glomeruli showed a few deposits in the mesangium (Fig. 3d, white arrow) as IgA nephropathy is present.[30,31] In addition, eNOSTg and eNOSTg/AK glomeruli showed mesangial deposits (Fig. 3f, h, white arrows).

In humans and mouse models, IgA nephropathy is characterized by mesangial immune complexes containing IgA, usually with C3, and variable IgG and/or IgM co-deposits.[32] IgA should be the dominant or at least codominant immunoglobulin by immunofluorescence. Deposits of C1q are infrequent in IgA nephropathy. In AK and eNOSTg/AK glomeruli, immunofluorescence studies confirmed the presence of mesangial IgA and C3 staining along with some mesangial IgM staining (Fig. 4A, upper and lower panel). Unexpectedly, eNOSTg glomeruli showed a similar pattern of staining (Fig. 4A, middle panel). Unstained sections of eNOSTg and eNOSTg/AK kidneys presented very minimal green fluorescence due to the expression of GFP (data not shown). In WT glomeruli, only nonspecific IgM staining was present and little or no IgG or C1q was detected in glomeruli from any group of mice. Since IgA nephropathy in AK mice is associated with elevated serum IgA levels,[30] circulating IgA was measured (Fig. 4B). IgA levels were increased in eNOSTg/AK mice (33.3 ± 2.73 mg/dl) similar to that reported in AK mice, whereas low levels of IgA were detected in WT mice. In eNOSTg mice, IgA levels were similar to WT.

3.4. Endothelial NOS is a chief source of superoxide generated in diabetic kidneys

To determine whether glomerular injury in eNOSTg and eNOSTg/AK mice was associated with enhanced superoxide generation, fresh sections of kidneys from all four groups were DHE stained as previously described[25] (Fig. 5A). Minimal background fluorescence was visualized in glomeruli of WT mice, whereas glomeruli in AK, eNOSTg and eNOSTg/AK mice exhibited enhanced DHE fluorescence in an ascending order. Quantification showed AK mice expressed 3.54 fold-, eNOSTg mice expressed 4.9 fold- and eNOSTg/AK mice expressed 5.2 fold-enhanced superoxide production (Fig. 5B, black bars). The level of superoxide production was significantly different ($^{*}p < 0.05$) between AK mice and both eNOSTg and eNOSTg/AK mice. Superoxide generation was not significantly different between eNOSTg and eNOSTg/AK mice. Prior incubation of kidney sections with 1 mM L-NAME, an inhibitor of NOS, blocked DHE fluorescence in AK, eNOSTg and eNOSTg/AK glomeruli, indicating that NOS was the predominant source of superoxide generated in eNOSTg and diabetic glomeruli (Fig. 5B, gray bars).

3.4.1. Increased peroxynitrite ($ONOO^-$) levels in AK, eNOSTg and eNOSTg/AK kidneys

Peroxynitrite is a reaction product of superoxide and nitric oxide. Under physiological conditions, nitrotyrosine, is formed exclusively from peroxynitrite and provides a marker of peroxynitrite activity. Protein modification by nitration of tyrosine to nitrotyrosine has been shown to correlate with elevated oxidative stress. We, therefore, examined kidney lysates for the presence of nitrotyrosine by western blotting. Immunoblot and quantitation shown in Fig. 5C panels (a) and (b) revealed a significant increase in nitrotyrosine levels (approximately 50-kDa protein band) in AK, eNOSTg and eNOSTg/AK kidney lysates relative to the levels observed in WT mice ($p < 0.001$). The overall nitrotyrosine levels were not significantly different ($p > 0.05$) between AK and eNOSTg mice. However, the level of nitrotyrosine was significantly higher ($p < 0.05$) in eNOSTg/AK mice compared to AK and eNOSTg mice.

4. Discussion

Endothelial NOS is the major NOS enzyme in vascular endothelial cells and a major source of NO in the kidney. In humans and rodent models, eNOS is increased in early diabetic nephropathy, but decreased with prolonged diabetes, leading to decreased endothelial NO and progression of disease.[15] Our previous studies in DKO mice showed that eNOS deficiency in diabetic mice increased renal injury, suggesting a protective role for eNOS-derived NO in diabetic renal disease.[4] To assess the effect of eNOS overexpression in the diabetic kidney, genetic crosses between eNOSTg mice and AK mice were performed to generate eNOSTg/AK mice. The AK mice are the optimal type 1 diabetic model due to a single nucleotide substitution in the insulin 2 gene (Ins^{C96Y}) which eliminates complex genetic traits.[23] The AK B6 strain was chosen for breeding with eNOSTg mice, which are on a B6 background.[26] Increased eNOS expression in the kidney of transgenic mice was confirmed by western blotting and immunostaining. Both AK and eNOSTg/AK mice showed elevated serum glucose levels, whereas levels in eNOSTg mice were similar to WT. AK mice are non-obese and body weight was not significantly different among the experimental groups. In AK mice, kidney size is reportedly increased at 24 weeks resulting in increased kidney to body weight ratio.[29] Although eNOSTg kidneys were normal in size, eNOSTg/AK mice showed kidney enlargement similar to AK mice.

Histologically, AK kidneys showed the expected diabetic morphology. Glomeruli in AK mice showed increased volume, matrix expansion, occasional early nodules and increased GBM thickness. No significant interstitial fibrosis was present. Unexpectedly, eNOSTg mice showed a similar increase in glomerular volume, matrix and GBM thickness but with additional features of glomerular injury including segmental

Fig. 1. Immunoblot analysis and immunohistochemistry of eNOS expression in kidney tissue. (A) Immunoblot shows total eNOS expression in kidney lysates prepared from WT, eNOSTg, AK and eNOSTg/AK mice. Kidneys isolated from eNOSTg and eNOSTg/AK mice showed an equivalent increase in total eNOS expression compared with WT mice ($^{*}p < 0.05$). A slightly lower level of total eNOS protein was detected in AK kidneys compared to WT ($^{**}p < 0.01$). A representative western blot from 6 independent experiments is shown (upper panel) ($n = 6$ mice/group). White line between eNOSTg and eNOSTg/AK lanes depicts deletion of a lane from the original image. (B) Band intensity was quantified by densitometry and the ratio of eNOS expression to non-specific protein (NS) loading control was used to determine fold-increase/decrease compared to WT group that was arbitrarily set at 1-fold (lower panel, bar graph). (C) Immunostained sections of kidneys from eNOSTg and eNOSTg/AK mice show increased eNOS expression in endothelial cells in glomerular capillaries and arterioles (brown color, arrows). In WT kidneys, an occasional glomerulus shows segmental endothelial staining and weak staining of endothelial cells in arterioles (arrows); significant eNOS expression could not be detected in glomeruli and arterioles of AK kidneys. (D) Low temperature – SDS-western blotting of kidney lysates from AK, eNOSTg and eNOSTg/AK mice showed monomers unlike the wild type mice which showed prominent dimer formation. Protein samples (150 μg protein/well) were subjected to electrophoresis under non-reducing conditions at a constant current of 20 mA. The gels were subsequently transferred on to a PVDF membrane and the eNOS dimers and monomers were detected using rabbit anti-eNOS antibody (Millipore). Human aortic endothelial cell lysates separated under non-reducing and reducing (lysate boiled with DTT) conditions were used as controls to confirm and validate experimental conditions that converts all dimers to monomers. The human cell lysates show the expected fast mobility of the dimer with its complete monomerization under reducing conditions.

Table 2
Renal Analysis.

Genotype	WT	AK	eNOSTg	eNOSTg/AK
Glomerular volume/μm^2	3477 (170.7)	4533 (241.7)*	4732 (413.7)*	4594 (95.18)*
Cellularity (cgs)[a]	38.21 (1.742)	45.50 (2.227)*	41.65 (1.986)	42.64 (3.056)
Matrix Fraction %	3.333 (0.3333)	6.800 (0.4899)**	6.600 (0.5099)**	7.667 (0.8819)***
Injury Index %[†]	0	1.10 (0.3317)**	7.50 (0.6708)***	20.00 (1.258)***
GBM thickness (μm)	0.196 (0.005)	0.262 (0.011)***	0.246 (0.002)**	0.265 (0.007)***
Fibrosis %	0.0350 (0.0201)	0.0586 (0.0270)	0.07175 (0.0134)	0.1043 (0.0188)

Data are mean (SEM), eNOSTg, AK, and eNOSTg/AK (n = 5–6) are compared with WT ($n = 3$) per group and each other using AVOVA followed by Fisher's Least Significant difference multiple comparisons t-tests.
* $p < 0.05$.
** $p < 0.01$.
*** $p < 0.001$ compared to WT.
† p < 0.01 comparing all pairs of groups (eNOSTg vs AK; eNOSTg/AK vs AK; and eNOSTg/AK vs eNOSTg.
[a] cgs: cell nuclei per glomerular cross-section.

mesangiolysis, denudation of endothelial cells, occasional microaneurysm formation and early sclerotic segments. Similar lesions were observed in eNOSTg/AK mice; however, overexpression of eNOS in the diabetic AK mice led to a significant increase in glomerular injury, with glomeruli showing more extensive mesangiolysis, endothelial denudation and segmental sclerotic lesions. Increased urine albumin/creatinine ratio correlated with renal damage observed in eNOSTg/AK mice, although values were not higher than in AK mice, likely due to variable ratios noted in the AK group. It is unlikely that blood pressure effects influenced renal morphology or function since a significant increase in systolic blood pressure was not detected in our AK or eNOSTg/AK mice at 24 weeks of age.[28] Whether blood pressure levels increased after 24 weeks of age and caused a detrimental effect cannot be excluded. Our data also suggest that hyperglycemia is not the only factor responsible for increased glomerular injury in eNOSTg/AK mice since these mice, similar to AK mice, were exposed to markedly elevated blood glucose levels for a prolonged period of time. Thus, a combination of eNOS overexpression and hyperglycemia likely contributed to the severity of renal lesions. In addition, insulin resistance has been linked to eNOS uncoupling and endothelial dysfunction in type-2 diabetes.[33] Although AK is a type-1 diabetic mouse, hyperglycemia-driven insulin resistance has been reported in this model.[34] Therefore, insulin resistance could also contribute to severity of renal lesions where eNOS is overexpressed.

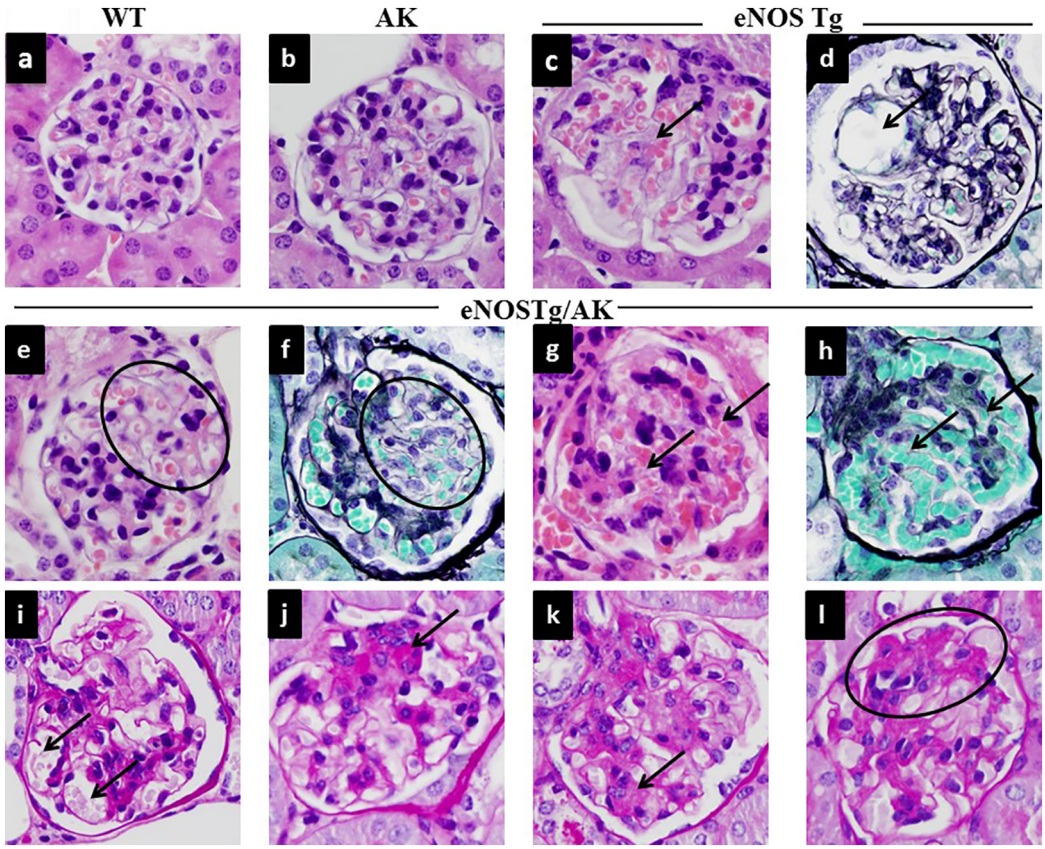

Fig. 2. Glomerular morphology. Representative images of glomerular morphology in WT, eNOSTg, AK and eNOSTg/AK mice. a) Normocellular glomerulus in WT mice. b) Increased glomerular volume and mild mesangial matrix expansion in AK mice. c) Segmental mesangiolysis and d) microaneruysm in eNOSTg mice (arrows). e-l) Spectrum of glomerular pathology in eNOSTg/AK mice showing: e, f) segmental mesangiolysis (circled) and g, h) global mesangiolysis (arrows); i) microaneurysms (arrows); j) perihilar hyaline (arrow); k) early nodule formation (arrow); l) sclerotic segments (circled). ($n = 3$–6 mice/group) Original magnification: x400 (a–c, e, g: H&E stain; d, f, h: methenamine silver stain; i-l: PAS stain).

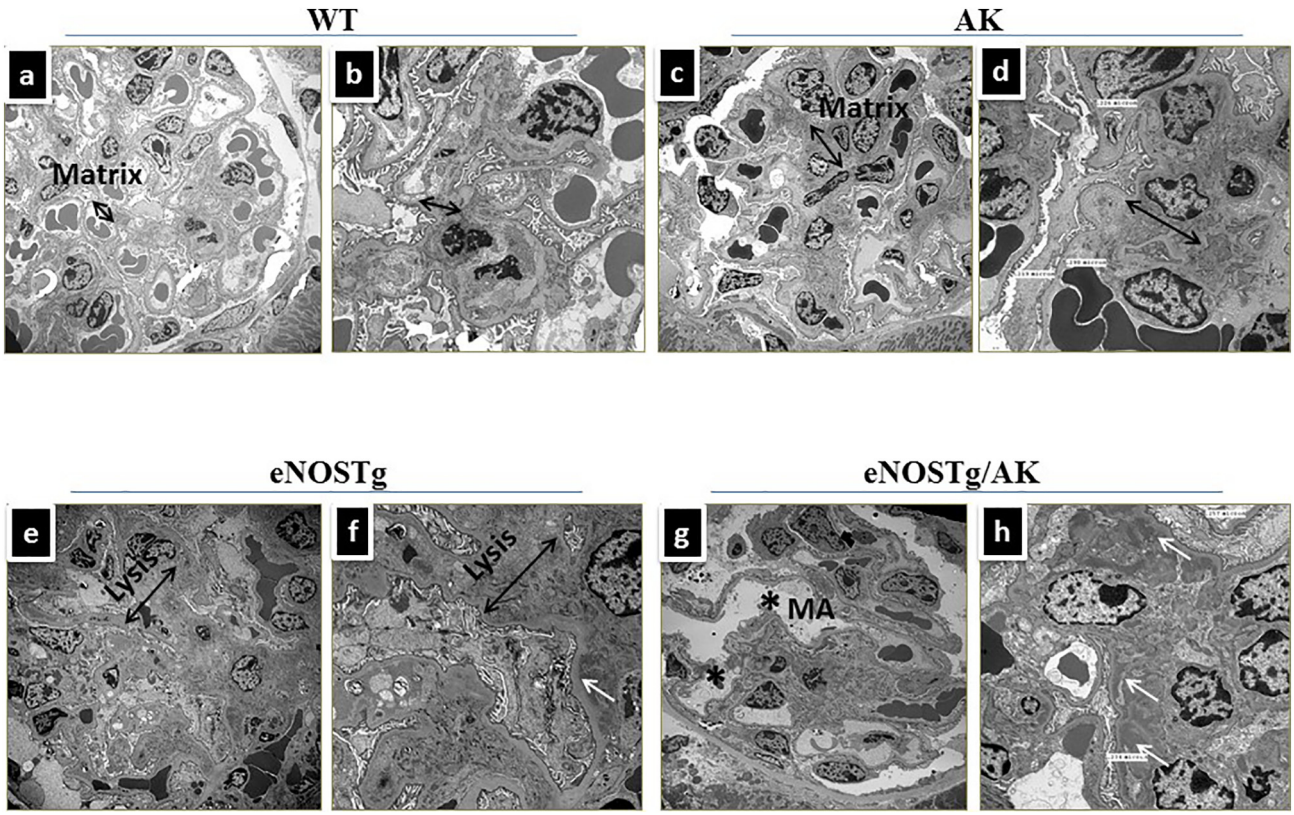

Fig. 3. Electron microscopic analysis of glomeruli. a, b) WT glomeruli show minimal mesangial matrix (arrow) in between capillaries. c, d) AK glomeruli show matrix expansion (arrows), thickened GBM and mesangial deposits (white arrow). e, f) eNOSTg glomeruli show segmental mesangiolysis with denudation of endothelial cells from the basement membrane (arrows). The matrix is expanded, GBM is thick and several mesangial deposits are identified (white arrow). g, h) eNOSTg/AK glomeruli show mesangiolysis with microaneurysm (MA) formation due to loss of anchoring of the basement membrane to the mesangium (asterisks). The matrix is expanded, the GBM is thick and mesangial deposits are identified (white arrows). Representative images are shown. (n = 3 mice/group) Original magnification: ×2500 in a, c, e, g; ×6000 in b, d, f, h.

Interestingly, mesangiolysis, microaneruysms, endothelial injury and impaired renal function which are prevalent features in eNOSTg/AK mice were also observed in our DKO mice with eNOS deficiency.[4] These findings indicate that overexpressing eNOS alone is not sufficient to ameliorate diabetic lesions, but paradoxically accelerates lesions. The spectrum of glomerular morphology in eNOSTg/AK mice resemble progressive stages observed in human type 1 diabetes where initially there is GBM thickening and matrix expansion, followed by mesangiolysis that leads to microaneurysms and nodular lesions.[35] Mesangiolysis may also heal to form perihilar hyaline and segmental sclerosis. Endothelial dysfunction and mesangiolysis occur in association with thrombotic microangiopathy and are implicated in the formation of microaneurysms and K—W nodules in diabetes.[36] Diabetic glomerular lesions may be associated with interstitial fibrosis and tubular atrophy and a trend toward increased fibrosis was observed in eNOSTg/AK kidneys. In addition to diabetic changes, immunofluorescence and EM studies revealed the presence of IgA nephropathy in AK mice that was recapitulated in eNOSTg/AK mice. Both groups of mice showed mesangial IgA deposits along with C3 and IgM co-deposits and elevated serum IgA levels, consistent with IgA nephropathy. AK mice have been shown to develop IgA nephropathy with elevated serum IgA levels at 20–30 weeks.[30,31] Superimposed IgA nephropathy has been reported in humans with diabetic nephropathy, with some patients showing increased circulating IgA.[37] Immune complex deposits with IgA were also identified in eNOSTg glomeruli. Whether circulating IgA levels increase with age in eNOSTg mice would be of interest.

Our findings indicate that increased glomerular injury in eNOSTg/AK mice is likely related to increased superoxide production. This is supported by our data showing increased superoxide generation in glomeruli of eNOSTg mice that was also observed in eNOSTg/AK glomeruli. The dramatic reduction of superoxide in response to L-NAME, an inhibitor of all three isoforms of NOS, clearly demonstrated that the major source of superoxide was NOS due to uncoupling. Since the eNOSTg and eNOSTg/AK mice used in this study overexpress eNOS, it is reasonable to consider that the major portion of superoxide generated is due to eNOS uncoupling relative to other NOS isoforms present in the kidney. Moreover, the reduced homodimer formation shown by western blotting using eNOS specific antibody corroborates this uncoupling process of eNOS. It is conceivable that increased superoxide in these glomeruli induced oxidation of BH4 resulting in uncoupling of eNOS which decreased NO bioavailability. Indeed, in separate studies evaluating macrovascular responses in the aorta, we showed that overexpression of eNOS in eNOSTg or eNOSTg/AK mice enhanced superoxide generation in endothelial cells and led to impaired vasorelaxation of thoracic aortae.[23] One limitation of the present study is that DHE fluorescence imaging in kidney sections to localize superoxide generation within the glomeruli was not accompanied by 2-hydroxyethidiuum measurements.[38] However, the increased peroxynitrite levels in the kidneys of eNOSTg/AK followed by eNOSTg and AK mice attests to the enhanced superoxide generation observed in these strains of mice.

Studies indicate that additional factors are required for eNOS to mediate beneficial effects. For example, when GTP cyclohydrolase 1 (GTPCH1) overexpressing mice were cross bred with eNOSTg mice, BH4 generation was enhanced in endothelial cells which restored NO production and reduced superoxide generation.[39] Kidokoro et al[40] demonstrated that cross breeding of GTPCH1 mice with type 1 diabetic mice restored intrarenal levels of BH4 which inhibited the progression of diabetic nephropathy. Dietary supplementation of L-Arginine or sepiapterin in diabetic mice[13] also showed beneficial effects of BH4 in improving eNOS activity and renal

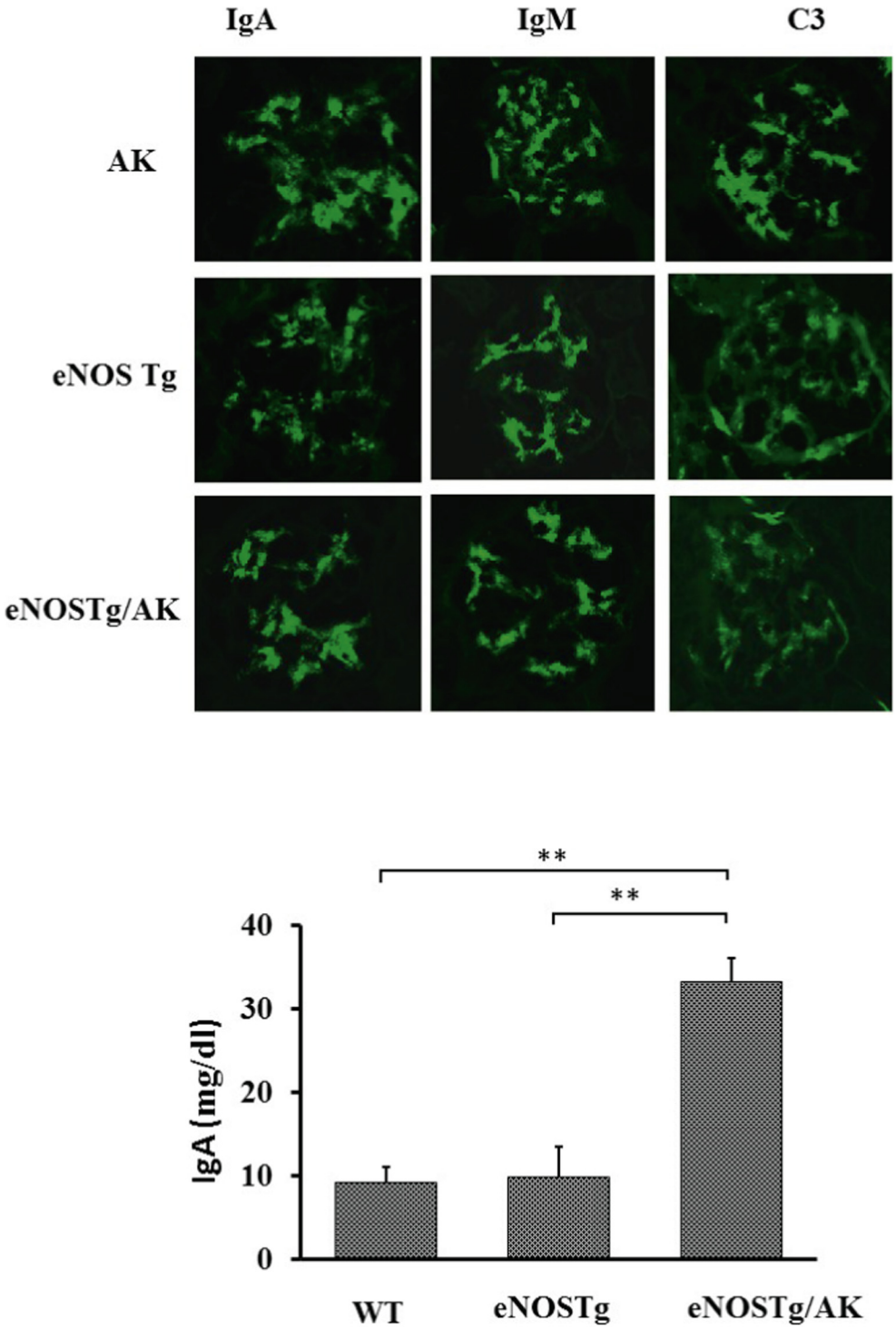

Fig. 4. Immunofluorescence studies of glomeruli. (A) A panel of immunofluorescent stains was performed on frozen kidney sections of WT, AK, eNOSTg and eNOSTg/AK mice. WT glomeruli showed nonspecific staining with IgM, consistent with entrapment (data not shown). AK, eNOSTg and eNOSTg/AK glomeruli showed mesangial IgA and C3 staining along with some mesangial IgM staining. These findings correlated with the presence of mesangial deposits on electron microscopy. Representative images are shown. (n = 3–4 mice/group) Original magnification: ×400, (B) Serum IgA analysis by ELISA. Compared with WT, eNOSTg/AK mice showed a 3-fold increase in circulating IgA levels. In contrast, eNOSTg mice showed IgA levels comparable to WT mice. Data represents mean (SEM), $^{**}p < 0.01$ (3–5 mice/group).

function. Taken together, results suggest that stoichiometric imbalance between expressed eNOS protein, limited local availability of substrate (L-Arginine) and cofactor (BH4) may have contributed to the accelerated renal disease in eNOSTg/AK mice.

In summary, our findings indicate for the first time that eNOS over-expression in type 1 diabetic mice exacerbates glomerular injury and progression of diabetic nephropathy. Results indicate that targeted expression of eNOS in combination with optimal levels of substrate and co- factor to endothelial cells within the kidney may enhance NO bioavailability and preserve renal function. The eNOSTg/AK mouse model provides a unique tool for understanding the mechanisms that control eNOS coupling and may lead to novel therapeutic strategies for enhancing eNOS activity to prevent the onset and progression of renal disease in diabetic patients.

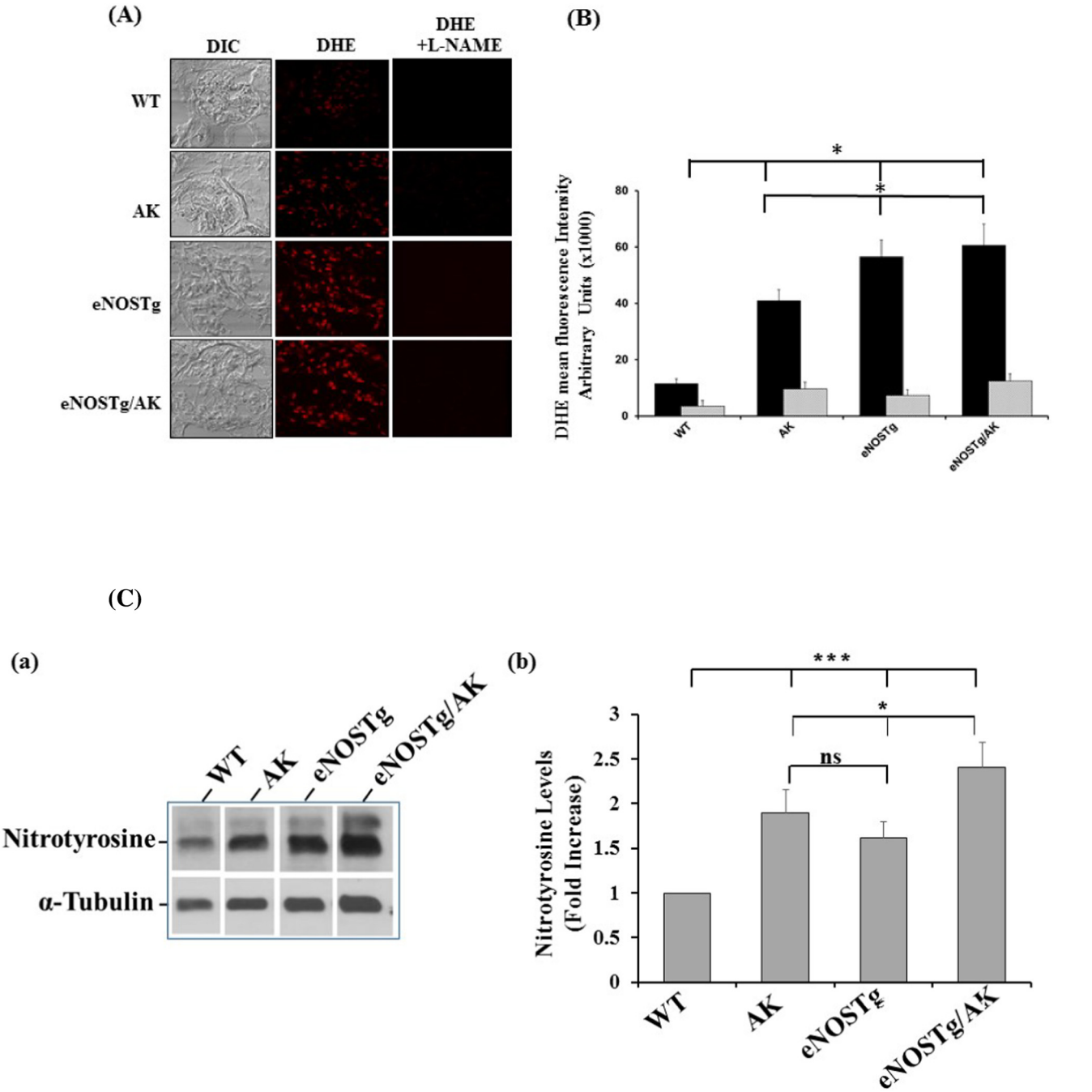

Fig. 5. Dihydroethidium (DHE) fluorescence in glomeruli. (A) Kidney sections from WT, AK, eNOSTg, eNOSTg/AK mice were incubated with 5 μM DHE for 30 min at 37 °C and subsequently visualized by fluorescence microscopy using rhodamine red to visualize DHE-positive fluorophore. WT glomeruli showed minimal background fluorescence. Glomeruli in AK, eNOSTg and the eNOSTg/AK mice exhibited increased DHE fluorescence relative to WT glomeruli. Incubation of sections with L-NAME significantly reduced DHE fluorescence in AK, eNOSTg and eNOSTg/AK glomeruli indicating NOS is the predominant source of superoxide generated in these glomeruli. (B) Quantitation of DHE fluorescence. Images were captured by Flowview1000 software and quantitation was performed using FIJI/ImageJ2 analysis software. Mean fluorescence intensity of 8–10 glomeruli in kidney sections (3mice/group) was determined and data are expressed as arbitrary units x 1000. L-NAME (1 mM) blocked a significant portion of DHE fluorescence (gray bars), indicating that NOS is a source of superoxide generation. Differential interference contrast (DIC) images show the unstained glomerular image. Data represents mean ± SEM. *, $p < 0.05$ denotes AK, eNOSTg and eNOSTg/AK are statistically significant compared to wild type and that eNOSTg and eNOSTg/AK are statistically significant compared to AK mice. (C) Panel (a) shows Nitrotyrosine levels in kidney lysates. Blots were probed with anti-nitrotyrosine or α-tubulin antibody. Representative immunoblots show an approximately 50 kDa nitrotyrosine protein band. Panel (b) shows band intensity. Band intensity was quantified by densitometry and the ratio of nitrotyrosine expression to α-tubulin loading control was used to determine fold-increase/decrease compared to WT group that was arbitrarily set at 1-fold. Compared to WT, increased nitrotyrosine levels were detected in eNOSTg/AK, eNOSTg and AK kidney lysates. Ns denotes no significant difference between AK and eNOSTg group. ***$p < 0.001$, *$p < 0.05$ ($n = 4$–6 mice/group).

Acknowledgements

We would like to thank Kathy Woodruff, Diane Horn, and Ngan Tran for technical help and Dr. Rene de Crom for providing resources for the breeding component of the project.

Funding

This study was supported by the NIH/NIDDK grant 5 RO1 DK096119 (SM), 5 R01 AG045040 (SLW) and the Office of the Assistant Secretary of Defense for Health Affairs through the Military Medical Research and

Development Program, Grant # CA140822 under Award No. W81XWH-14-PRCRP-IA (MN).

References

1. Martinez-Castelao A, Navarro-Gonzalez JF, Gorriz JL, de Alvaro F. The concept and the epidemiology of diabetic nephropathy have changed in recent years. J Clin Med 2015;4:1207-16.
2. Erdely A, Freshour G, Maddox DA, Olson JL, Samsell L, Baylis C. Renal disease in rats with type 2 diabetes is associated with decreased renal nitric oxide production. Diabetologia 2004;47:1672-6.
3. Hink U, Li H, Mollnau H, et al. Mechanisms underlying endothelial dysfunction in diabetes mellitus. Circ Res 2001;88:E14-22.
4. Mohan S, Reddick RL, Musi N, et al. Diabetic eNOS knockout mice develop distinct macro- and microvascular complications. Lab Invest 2008;88:515-28.
5. Han KH, Lim JM, Kim WY, Kim H, Madsen KM, Kim J. Expression of endothelial nitric oxide synthase in developing rat kidney. Am J Physiol Ren Physiol 2005;288: F694-702.
6. Ignarro LJ, Buga GM, Wei LH, Bauer PM, Wu G, del Soldato P. Role of the arginine-nitric oxide pathway in the regulation of vascular smooth muscle cell proliferation. Proc Natl Acad Sci U S A 2001;98:4202-8.
7. Mellion BT, Ignarro LJ, Ohlstein EH, Pontecorvo EG, Hyman AL, Kadowitz PJ. Evidence for the inhibitory role of guanosine 3′, 5′-monophosphate in ADP-induced human platelet aggregation in the presence of nitric oxide and related vasodilators. Blood 1981;57:946-55.
8. Deng A, Baylis C. Locally produced EDRF controls preglomerular resistance and ultrafiltration coefficient. Am J Physiol 1993;264:F212-5.
9. Mattson DL, Roman RJ, Cowley Jr AW. Role of nitric oxide in renal papillary blood flow and sodium excretion. Hypertension 1992;19:766-9.
10. Zatz R, de Nucci G. Effects of acute nitric oxide inhibition on rat glomerular microcirculation. Am J Physiol 1991;261:F360-3.
11. Crabtree MJ, Smith CL, Lam G, Goligorsky MS, Gross SS. Ratio of 5,6,7,8-tetrahydrobiopterin to 7,8-dihydrobiopterin in endothelial cells determines glucose-elicited changes in NO vs. superoxide production by eNOS. Am J Physiol Heart Circ Physiol 2008;294:H1530-40.
12. Komers R, Anderson S. Paradoxes of nitric oxide in the diabetic kidney. Am J Physiol Ren Physiol 2003;284:F1121-37.
13. Cheng H, Wang H, Fan X, Paueksakon P, Harris RC. Improvement of endothelial nitric oxide synthase activity retards the progression of diabetic nephropathy in db/db mice. Kidney Int 2012;82:1176-83.
14. Nakagawa T, Sato W, Glushakova O, et al. Diabetic endothelial nitric oxide synthase knockout mice develop advanced diabetic nephropathy. J Am Soc Nephrol 2007;18:539-50.
15. Takahashi T, Harris RC. Role of endothelial nitric oxide synthase in diabetic nephropathy: lessons from diabetic eNOS knockout mice. J Diabetes Res 2014;2014, 590541.
16. Zhao HJ, Wang S, Cheng H, et al. Endothelial nitric oxide synthase deficiency produces accelerated nephropathy in diabetic mice. J Am Soc Nephrol 2006;17:2664-9.
17. Badal SS, Danesh FR. Strategies to reverse endothelial dysfunction in diabetic nephropathy. Kidney Int 2012;82:1151-4.
18. Savard S, Lavoie P, Villeneuve C, Agharazii M, Lebel M, Lariviere R. eNOS gene delivery prevents hypertension and reduces renal failure and injury in rats with reduced renal mass. Nephrol Dial Transplant 2012;27:2182-90.
19. Jones SP, Greer JJ, Kakkar AK, et al. Endothelial nitric oxide synthase overexpression attenuates myocardial reperfusion injury. Am J Physiol Heart Circ Physiol 2004;286:H276-82.
20. Kawashima S, Yamashita T, Ozaki M, et al. Endothelial NO synthase overexpression inhibits lesion formation in mouse model of vascular remodeling. Arterioscler Thromb Vasc Biol 2001;21:201-7.
21. Yamashita T, Kawashima S, Ohashi Y, et al. Resistance to endotoxin shock in transgenic mice overexpressing endothelial nitric oxide synthase. Circulation 2000;101: 931-7.
22. Brunner F, Maier R, Andrew P, Wolkart G, Zechner R, Mayer B. Attenuation of myocardial ischemia/reperfusion injury in mice with myocyte-specific overexpression of endothelial nitric oxide synthase. Cardiovasc Res 2003;57:55-62.
23. Yoshioka M, Kayo T, Ikeda T, Koizumi A. A novel locus, Mody4, distal to D7Mit189 on chromosome 7 determines early-onset NIDDM in nonobese C57BL/6 (Akita) mutant mice. Diabetes 1997;46:887-94.
24. Breyer MD, Bottinger E, Brosius III FC, et al. Mouse models of diabetic nephropathy. J Am Soc Nephrol 2005;16:27-45.
25. Krishnan M, Janardhanan P, Roman L, et al. Enhancing eNOS activity with simultaneous inhibition of IKKbeta restores vascular function in Ins2(Akita+/−) type-1 diabetic mice. Lab Invest 2015;95:1092-104.
26. van Haperen R, Cheng C, Mees BM, et al. Functional expression of endothelial nitric oxide synthase fused to green fluorescent protein in transgenic mice. Am J Pathol 2003;163:1677-86.
27. Yang YM, Huang A, Kaley G, Sun D. eNOS uncoupling and endothelial dysfunction in aged vessels. Am J Physiol Heart Circ Physiol 2009;297:H1829-36.
28. Chandra SB, Mohan S, Ford BM, et al. Targeted overexpression of endothelial nitric oxide synthase in endothelial cells improves cerebrovascular reactivity in Ins2Akita-type-1 diabetic mice. J Cereb Blood Flow Metab 2016;36:1135-42.
29. Gurley SB, Mach CL, Stegbauer J, et al. Influence of genetic background on albuminuria and kidney injury in Ins2(+/C96Y) (Akita) mice. Am J Physiol Ren Physiol 2010;298:F788-95.
30. Haseyama T, Fujita T, Hirasawa F, et al. Complications of IgA nephropathy in a non-insulin-dependent diabetes model, the Akita mouse. Tohoku J Exp Med 2002;198: 233-44.
31. Sanchez AP, Zhao J, You Y, Decleves AE, Diamond-Stanic M, Sharma K. Role of the USF1 transcription factor in diabetic kidney disease. Am J Physiol Ren Physiol 2011;301:F271-9.
32. Suzuki H, Suzuki Y, Novak J, Tomino Y. Development of animal models of human IgA nephropathy. Drug Discov Today Dis Model 2014;11:5-11.
33. Katakam PV, Snipes JA, Steed MM, Busija DW. Insulin-induced generation of reactive oxygen species and uncoupling of nitric oxide synthase underlie the cerebrovascular insulin resistance in obese rats. J Cereb Blood Flow Metab 2012;32:792-804.
34. Hong EG, Jung DY, Ko HJ, et al. Nonobese, insulin-deficient Ins2Akita mice develop type 2 diabetes phenotypes including insulin resistance and cardiac remodeling. Am J Physiol Endocrinol Metab 2007;293:E1687-96.
35. Stout LC, Kumar S, Whorton EB. Focal mesangiolysis and the pathogenesis of the Kimmelstiel-Wilson nodule. Hum Pathol 1993;24:77-89.
36. Paueksakon P, Revelo MP, Ma LJ, Marcantoni C, Fogo AB. Microangiopathic injury and augmented PAI-1 in human diabetic nephropathy. Kidney Int 2002;61:2142-8.
37. Fiorentino M, Bolignano D, Tesar V, et al. Renal biopsy in patients with diabetes: a pooled meta-analysis of 48 studies. Nephrol Dial Transplant 2017;32:97-110.
38. Dikalov S, Griendling KK, Harrison DG. Measurement of reactive oxygen species in cardiovascular studies. Hypertension 2007;49:717-27.
39. Alp NJ, Mussa S, Khoo J, et al. Tetrahydrobiopterin-dependent preservation of nitric oxide-mediated endothelial function in diabetes by targeted transgenic GTP-cyclohydrolase I overexpression. J Clin Invest 2003;112:725-35.
40. Kidokoro K, Satoh M, Channon KM, Yada T, Sasaki T, Kashihara N. Maintenance of endothelial guanosine triphosphate cyclohydrolase I ameliorates diabetic nephropathy. J Am Soc Nephrol 2013;24:1139-50.